Optics Letters

Real-time and high-precision interrogation of a linearly chirped fiber Bragg grating sensor array based on dispersive time delay and optical pulse compression

Bin Wang,[1,2] Ping Lu,[3] Stephen J. Mihailov,[3] Xinyu Fan,[2] and Jianping Yao[1,*]

[1]Microwave Photonics Research Laboratory, School of Electrical Engineering and Computer Science, University of Ottawa, Ontario K1N 6N5, Canada
[2]State Key Laboratory of Advanced Optical Communication Systems and Networks, Department of Electronic Engineering, Shanghai Jiao Tong University, Shanghai 200240, China
[3]National Research Council Canada, Ottawa, Ontario K1A 0R6, Canada
*Corresponding author: jpyao@eecs.uottawa.ca

Received 15 April 2019; revised 26 May 2019; accepted 28 May 2019; posted 3 June 2019 (Doc. ID 365152); published 18 June 2019

A novel technique to achieve real-time and high-precision interrogation of a linearly chirped fiber Bragg (LCFBG) grating sensor array based on dispersive time delay and optical pulse compression is proposed and experimentally demonstrated. In the proposed system, an ultra-short optical pulse is launched into an LCFBG sensor array consisting of N identical LCFBGs, to produce N reflected pulses with their time delay changes corresponding to the strain or temperature changes. The reflected pulses are sent to another LCFBG having an opposite dispersion coefficient to achieve optical pulse compression to improve the measurement accuracy. A proof-of-concept experiment is demonstrated. A 2 × 3 LCFBG sensor array using six identical LCFBGs is implemented, and the performance is evaluated experimentally. The sensing speed can be as high as 48.6 MHz, and the sensing accuracy can be as high as 0.26 με for strain and 0.045°C for temperature.

https://doi.org/10.1364/OL.44.003246

Fiber Bragg grating (FBG) sensors have been intensively investigated and widely used for the last few decades due to their distinctive advantages, such as compact size, light weight, immunity to electromagnetic interference, and large-scale multiplexing capability. In an FBG sensor, the measurands, such as temperature, strain, and/or pressure, are encoded in the wavelength as a wavelength shift [1], and various interrogation techniques have been proposed to monitor the wavelength shift. Among the numerous interrogation techniques, the use of an optical spectrum analyzer is the simplest solution, but the measurement speed is relatively slow and the resolution is poor. To improve the measurement speed, one may use a wavelength discriminator to convert the wavelength change to optical power change [2–4], but the measurement accuracy is limited, since the power shift of the laser source or the spectral drift of the wavelength discriminator will cause output power drift, leading to incorrect wavelength measurement.

To increase the measurement accuracy and resolution, a solution is to convert the wavelength change to a microwave frequency shift or a time shift in the microwave domain—a technique termed microwave photonic sensing [5]. For example, the wavelength shift of an FBG can be translated to a microwave frequency change using an optoelectronic oscillator [6–8], or a microwave photonic filter [9]. The wavelength change can also be converted to a time shift of a microwave pulse based on spectral shaping and wavelength-to-time mapping [10–15]. The frequency or time shift in the microwave domain can be measured at a much higher speed and accuracy; thus, the entire system performance in terms of speed, accuracy, and resolution is highly improved. The major limitation of these approaches is that a high-speed digital signal processor (DSP) is needed to perform spectral analysis for frequency measurement or pulse compression for time shift measurement, which may impose a stringent speed requirement for the DSP. Recently, a high-precision linearly chirped FBG (LCFBG) sensor interrogated using a linearly chirped optical waveform has been proposed [16], which provides a measurement speed of 1 MHz and a resolution of 0.25 με. However, the ultimate sensing speed of this method is limited by the sweeping speed of the laser source, and a large-scale multiplexing is difficult to realize.

In this Letter, we propose and demonstrate a novel technique to achieve real-time interrogation of an LCFBG sensor array at a high speed with high resolution based on dispersive time delay and optical pulse compression. In the proposed system, a mode-locked laser (MLL) source is used to generate an optical pulse with a broad optical spectrum, which is sent to an LCFBG sensor array where the spectrum is shaped by the LCFBGs with the sensing information encoded as spectrum shifts. The reflected pulses are then sent to another LCFBG

having an opposite dispersion coefficient to achieve optical pulse compression to improve the measurement accuracy. As a demonstration, a 2 × 3 LCFBG sensor array is fabricated and is employed to realize quasi-distributed sensing. The LCFBGs are identical with identical spectral responses, but the physical locations are different; thus, the optical pulses reflected by the LCFBGs can be identified by their time delays. In the proposed technique, optical pulse compression is implemented in the optical domain, and the distributed sensing information is obtained from the time delays of the compressed pulses. Since the pulse compression is performed directly in the optical domain, high-speed and high-accuracy interrogation without the need for a high-speed DSP is realized.

Figure 1 illustrates the principle of the proposed technique in which a single LCFBG is used as the sensor. An ultra-short pulse generated by an MLL source is launched into the LCFBG with a dispersion coefficient $\ddot{\Phi}$. When a strain is applied to the LCFBG, or the ambient temperature is changed, the reflection spectrum of the LCFBG will have a wavelength shift $\Delta\lambda$ (green dashed line). Due to the dispersion effect in the LCFBG, the reflected pulse will have a time delay Δt (point B, blue dashed line). In this case, the wavelength shift induced by the strain or temperature change is encoded in the time shift of the reflected pulse. In addition to the time shift, the reflected pulse is also temporally stretched (point B, blue solid line) due to the dispersion effect of the LCFBG, which would deteriorate the SNR and the measurement resolution. To solve this problem, another LCFBG with an opposite dispersion coefficient $-\ddot{\Phi}$ is incorporated into the system to compress the stretched pulse.

Assume the optical pulse generated by the MLL source is $i(t)$, and the impulse response of the LCFBG is $h(t)$. The reflected pulse is a convolution between the input pulse $i(t)$ and the impulse response $h(t)$, given by

$$e(t) = i(t) * h(t). \tag{1}$$

Equation (1) can be expressed in the frequency domain:

$$E(\omega) = I(\omega)H(\omega), \tag{2}$$

where $E(\omega)$, $I(\omega)$, and $H(\omega)$ are the Fourier transforms of $e(t)$, $i(t)$, and $h(t)$, respectively. The impulse response of an LCFBG in the frequency domain can be given as [17]

$$H(\omega) = R\exp\left(\frac{j\ddot{\Phi}\omega^2}{2}\right), \tag{3}$$

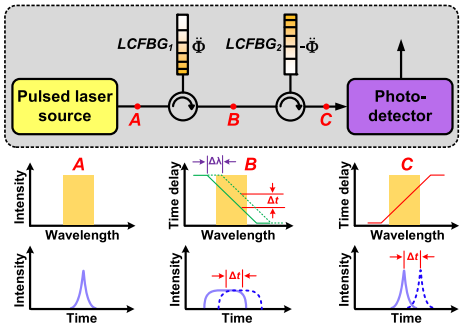

Fig. 1. Principle of the proposed interrogation technique based on dispersive time delay and optical pulse compression. LCFBG, linearly chirped fiber Bragg grating.

where R is the reflectivity of the LCFBG, which is assumed to be constant within the bandwidth. Then Eq. (2) can be rewritten as

$$E(\omega) = RI(\omega)\exp\left(\frac{j\ddot{\Phi}\omega^2}{2}\right). \tag{4}$$

When the LCFBG is stretched or heated, a wavelength shift will be generated, and the reflected pulse in the frequency domain is given by

$$\begin{aligned} E'(\omega) &= RI(\omega)\exp\left(\frac{j\ddot{\Phi}(\omega-\Delta\omega)^2}{2}\right) \\ &= R'I(\omega)\exp\left(\frac{j\ddot{\Phi}\omega^2}{2}\right)\exp(-j\omega\ddot{\Phi}\Delta\omega), \end{aligned} \tag{5}$$

where $R' = R\exp(j\ddot{\Phi}(\Delta\omega)^2/2)$, and $\Delta\omega$ is the frequency shift of the grating spectrum induced by the strain or temperature change. Subsequently, the reflected pulse is launched into another LCFBG with an opposite dispersion coefficient $-\ddot{\Phi}$, and the output pulse can be expressed as

$$\begin{aligned} E_{\text{out}}(\omega) &= E'(\omega)\exp\left(\frac{-j\ddot{\Phi}\omega^2}{2}\right) \\ &= R'I(\omega)\exp(-j\ddot{\Phi}\Delta\omega\omega). \end{aligned} \tag{6}$$

By applying the inverse Fourier transform to both sides of Eq. (6), we have the output pulse in the time domain given by

$$i_{\text{out}}(t) = R'i(t-\ddot{\Phi}\Delta\omega). \tag{7}$$

According to Eq. (7), the wavelength shift of the LCFBG can be measured by recording the time delay of the reflected pulse.

In order to realize quasi-distributed sensing, an LCFBG sensor array is prepared by connecting N identical weak LCFBGs at different physical locations, as shown in Fig. 2. Then the output pulse sequence can be expressed as

$$i_{\text{out}}^N = \sum_{k=1}^{N} i_{\text{out}}\left(t-\frac{2nL_k}{c}\right), \tag{8}$$

where n is the refractive index of the fiber core, c is the velocity of light in vacuum, and L_k is the location of the k-th LCFBG. By properly choosing the locations of the LCFBGs, a large-scale multiplexed sensing system can be realized.

The feasibility of the proposed technique is experimentally validated based on the experimental setup shown in Fig. 2. An MLL source (IMRA Femtolite 780 Model B-4-FC-PD) is used to generate an optical pulse train with an individual pulse having a full-width at half-maximum (FWHM) of 394 fs at a central wavelength of 1558 nm and a repetition rate of 48.6 MHz. The ultra-short optical pulse is then launched into an optical bandpass filter (BPF, Finisar Waveshaper 4000S) with a bandwidth of 0.7 nm to make the pulse have a narrow spectral width. The pulse width is extended to 5 ps. Subsequently, the optical pulse is injected into a 2 × 3 LCFBG sensor array. All the LCFBGs are identical and have a length of 12 cm, a central wavelength of 1558.3 nm, a bandwidth of 1.5 nm, a dispersion coefficient of −700 ps/nm, and a reflectivity of ∼20%. The LCFBGs are fabricated plane-by-plane by using a Ti:sapphire regeneratively amplified femtosecond infrared (fs-IR) laser (Spitfire, Coherent). The fs-IR laser operates at the wavelength of 800 nm with a repetition rate of about 1000 Hz and a pulse duration of 120 fs. To avoid sensing

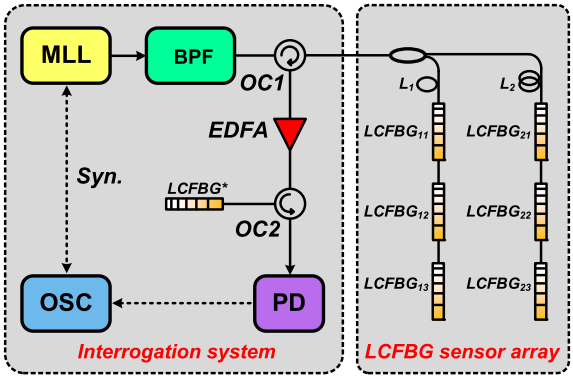

Fig. 2. Experimental setup of the proposed sensing system. MLL, mode-locked laser; BPF, optical bandpass filter; OC, optical circulator; EDFA, erbium-doped fiber amplifier; PD, photodetector; OSC, oscilloscope.

ambiguity, the locations of the LCFBGs are chosen such that the time separation of the pulses reflected from two adjacent LCFBGs is larger than the strain or temperature induced time shift. An erbium-doped fiber amplifier (EDFA) is utilized to increase the power of the reflected pulses. An identical LCFBG (LCFBG*) that is connected reversely to have an opposite dispersion coefficient of 700 ps/nm, is incorporated to compress the reflected pulses. Finally, the compressed optical pulses are fed into a 20 GHz photodetector (PD), and a real-time oscilloscope is used to record the electrical waveforms.

Figures 3(a) and 3(b) shows a reflected pulse from one LCFBG ($LCFBG_{11}$) without and with pulse compression, respectively. Due to the large dispersion of the LCFBG, the reflected pulse is largely stretched, and the pulse width is measured to be 480 ps, which leads to a poor measurement resolution. After passing through an LCFBG with an opposite dispersion coefficient, the pulse is compressed. The zoom-in view of the compressed pulse is shown in the inset in Fig. 3(b). The FWHM of the compressed pulse is measured to be 27 ps.

A strain sensing experiment is first performed. In the experiment, only $LCFBG_{13}$ is stretched, and the ambient temperature is kept unchanged. As shown in Fig. 4(a), the pulses reflected by the six LCFBGs have different time delays, since they are located at different physical positions. Figures 4(b) and 4(c) show the reflected pulses from $LCFBG_{21}$ and $LCFBG_{13}$. It can be observed that when no strain is applied, the time delay of the reflected pulse is kept unchanged. When an increased strain is applied to the LCFBG, the time delay of the reflected pulse is

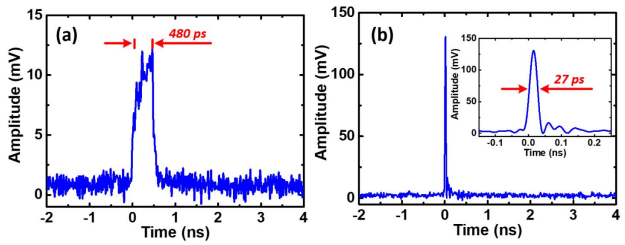

Fig. 3. Reflected pulse (a) without and (b) with pulse compression. The inset is the zoom-in view of the compressed pulse.

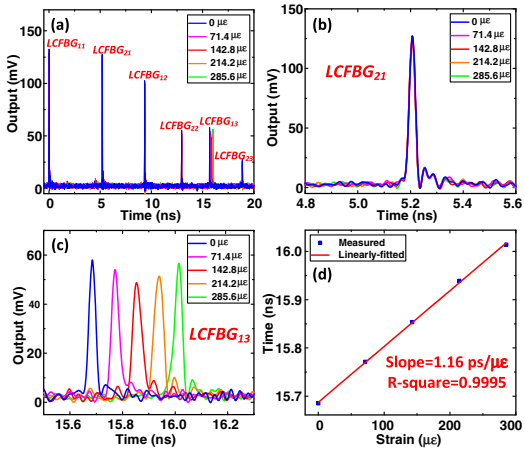

Fig. 4. (a) Measured pulses reflected by the LCFBG sensor array when $LCFBG_{13}$ is stretched. (b) Reflected pulse from $LCFBG_{21}$. (c) Reflected pulse from $LCFBG_{13}$. (d) Relationship between the strain and time delay of the pulse reflected from $LCFBG_{13}$ when the temperature is kept unchanged.

increased accordingly. Figure 4(d) shows the relationship between the strain and the time delay of the reflected pulse. It can be observed that the time delay changes linearly with the strain, and the strain sensitivity is calculated to be 1.16 ps/με with an *R*-square value of 0.9995.

Then a temperature sensing experiment is performed. In the experiment, $LCFBG_{22}$ and $LCFBG_{23}$ are heated, while the other LCFBGs are controlled at a fixed room temperature (25°C). The reflected pulses are shown in Fig. 5(a). Figure 5(b) shows the reflected pulse from $LCFBG_{12}$. It can be seen that the time delay of the reflected pulse remains unchanged, since the temperature is fixed. Figure 5(c) shows the reflected pulse from $LCFBG_{22}$. It can be observed that the time delay of the pulse is increasing when the temperature is changed. Figure 5(d) shows a linear relationship between the temperature and time delay of the reflected pulse from $LCFBG_{22}$. The temperature sensitivity is calculated to be 6.68 ps/°C, and the *R*-square value is 0.9998. The pulse reflected from $LCFBG_{23}$ is shown in Fig. 5(e), and Fig. 5(f) gives the relationship between the temperature and time delay of the pulse reflected by $LCFBG_{23}$. The temperature sensitivity is calculated to be 6.81 ps/°C with an *R*-square value of 0.9990.

Finally, the measurement accuracy of the proposed system is evaluated. In the measurements, 200 reflected pulse sequences are recorded by using the real-time OSC. All the LCFBGs are not experiencing strain and temperature change. The histograms to show the time delay fluctuations are shown in Fig. 6. The standard deviations of the time delay fluctuations of the reflected pulses from $LCFBG_{11}$, $LCFBG_{21}$, and $LCFBG_{12}$ are calculated to be 0.3 ps, which corresponds to a measurement accuracy of 0.26 με for strain and 0.045°C for temperature. For $LCFBG_{22}$, $LCFBG_{13}$, and $LCFBG_{23}$, the standard deviations of the time delay fluctuations are increased to be 0.4, 0.5, and 0.8 ps, respectively, which means a deteriorated measurement accuracy. The reason for the deteriorated accuracy is the decrease in amplitude of the reflected pulses, which is mainly caused by the insertion loss of the LCFBGs. To improve the measurement accuracy, an

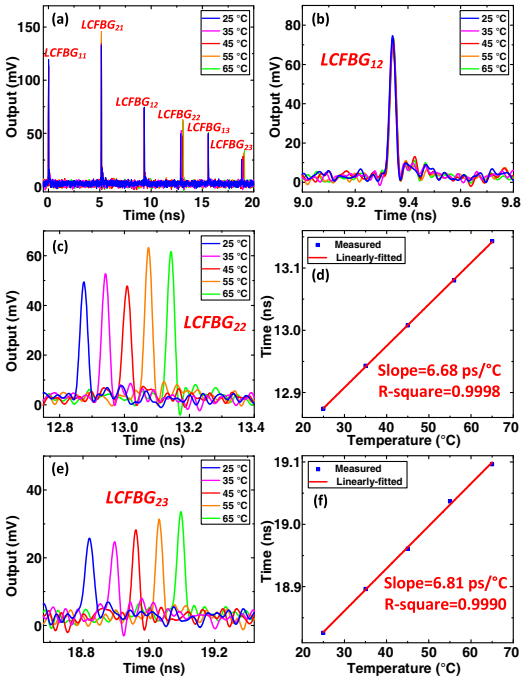

Fig. 5. (a) Measured pulses reflected from the LCFBG sensor array when $LCFBG_{22}$ and $LCFBG_{23}$ are heated. (b) Reflected pulse from $LCFBG_{12}$ with no temperature change. (c) Reflected pulse from $LCFBG_{22}$ under different temperature values. (d) Relationship between the temperature and time delay of the pulse reflected from $LCFBG_{22}$. (e) Reflected pulse from $LCFBG_{23}$ under different temperature values. (f) Relationship between temperature and time delay of the pulse reflected from $LCFBG_{23}$.

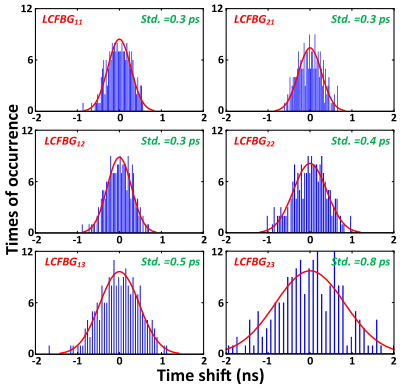

Fig. 6. Histograms of the time delay fluctuations of the reflected pulses when no strain is applied to the LCFBGs and the ambient temperature remains unchanged. The measurement number is 200.

effective method is to use LCFBGs with lower insertion loss as the sensor elements.

In the proposed system, the strain and temperature sensitivity of an LCFBG element is determined by the dispersion coefficient of the LCFBG. In our experiments, the LCFBGs are identical, and each has a dispersion coefficient of 700 ps/nm. We believe that the sensitivity can be improved simply by using LCFBGs with a higher dispersion coefficient. As a demonstration of quasi-distributed sensing, six LCFBGs with a reflectivity of ~20% are used in the experiments. Here the number of the sensing units (LCFBGs) is limited by the insertion loss of the LCFBGs. More sensing units can be multiplexed when LCFBGs with lower reflectivity and insertion loss are utilized. The maximum measurement distance of the system is about 2.1 m, which is limited by the repetition rate of the MLL (48.6 MHz). We believe that a longer measurement distance can be realized by using an MLL with a lower repetition rate. The current spatial resolution for LCFBG locating is about 5 mm, which is determined by the bandwidth of the PD (20 GHz). A higher spatial resolution can be realized by using a PD with a larger bandwidth.

In conclusion, we have proposed and experimentally demonstrated a novel technique for real-time and high-precision interrogation of an LCFBG sensor array based on dispersion time delay and optical pulse compression. The key of the approach was to transfer the measurands, such as strain and temperature, to the time delay of the pulses reflected by the LCFBG sensor array. The resolution of the system was improved by optical pulse compression, which was implemented in the optical domain; thus, ultra-high-speed interrogation without the need for high-speed DSP to perform pulse compression in the electrical domain was realized. As a demonstration, a 2 × 3 LCFBG sensor array was fabricated, and its use for quasi-distributed sensing was performed. The sensing speed can be as high as 48.6 MHz, and the measurement accuracy was as high as 0.26 με for strain and 0.045°C for temperature.

Funding. Natural Sciences and Engineering Research Council of Canada (NSERC); China Scholarship Council (CSC) (201706230127).

REFERENCES

1. A. D. Kersey, M. A. Davis, H. J. Patrick, M. LeBlanc, K. P. Koo, C. G. Askins, M. A. Putnam, and E. J. Friebele, J. Lightwave Technol. **15**, 1442 (1997).
2. U. Tiwari, K. Thyagarajan, M. R. Shenoy, and S. C. Jain, IEEE Sens. J. **13**, 1315 (2013).
3. A. D. Kersey, T. A. Berkoff, and W. W. Morey, Opt. Lett. **18**, 1370 (1993).
4. Y. Nakazaki and S. Yamashita, Opt. Express **17**, 8310 (2009).
5. J. P. Yao, Fiber Integrated Opt. **34**, 204 (2015).
6. F. Kong, W. Li, and J. P. Yao, Opt. Lett. **38**, 2611 (2013).
7. X. H. Zou, X. K. Liu, W. Z. Li, P. X. Li, W. Pan, L. S. Yan, and L. Y. Shao, IEEE J. Quantum Electron. **52**, 1 (2016).
8. J. P. Yao, J. Lightwave Technol. **35**, 3489 (2017).
9. O. Xu, J. Zhang, and J. P. Yao, Opt. Lett. **41**, 4859 (2016).
10. M. L. Dennis, M. A. Putnam, J. U. Kang, T. Tsai, I. N. Duling, and E. J. Friebele, Opt. Lett. **22**, 1362 (1997).
11. H. Xia, C. Wang, S. Blais, and J. P. Yao, J. Lightwave Technol. **28**, 254 (2010).
12. W. Liu, M. Li, C. Wang, and J. P. Yao, J. Lightwave Technol. **29**, 1239 (2011).
13. W. Liu, W. Li, and J. P. Yao, IEEE Photonics Technol. Lett. **23**, 1340 (2011).
14. H. Deng, P. Lu, S. Mihailov, and J. P. Yao, J. Lightwave Technol. **36**, 5587 (2018).
15. J. Liu, P. Lu, S. Mihailov, M. Wang, and J. P. Yao, Opt. Lett. **44**, 379 (2019).
16. Y. Wang, J. Zhang, O. Coutinho, and J. Yao, Opt. Lett. **40**, 4923 (2015).
17. J. Zhang and J. P. Yao, Optica **1**, 64 (2014).